Ocean Engineering 165 (2018) 399–409

Contents lists available at ScienceDirect

Ocean Engineering

journal homepage: www.elsevier.com/locate/oceaneng

Short communication

Robust H_2 optimal depth control of an autonomous underwater vehicle with output disturbances and time delay

Lei Qiao[a], Shitao Ruan[a], Guoqing Zhang[a,b], Weidong Zhang[a,*]

[a] Department of Automation, Shanghai Jiao Tong University, Shanghai 200240, China
[b] Navigation College, Dalian Maritime University, Dalian, Liaoning 116026, China

ARTICLE INFO

Keywords:
Autonomous underwater vehicle (AUV)
Depth control
Robust H_2 optimal control
Output disturbances
Time delay

ABSTRACT

This paper proposes a robust H_2 optimal control strategy for the depth-plane motion of an autonomous underwater vehicle (AUV) in the presence of output disturbances and time delay. The six degrees of freedom nonlinear kinematic and dynamic equations of motion of the vehicle are firstly described. The depth-plane linearization of the vehicle equations of motion is then derived for efficient controller design from the practical point of view. Using this linearized and reduced-order model, a robust H_2 optimal control method is designed. The designed control method takes into account both the output disturbances and time delay and provides suitable control action for desired tracking. The robust stability and robust performance of the proposed control method with respect to the model uncertainties are discussed. Simulation studies demonstrate that the proposed robust H_2 optimal control strategy has remarkable performance and provides higher tracking accuracy, better output disturbances rejection ability, stronger robustness against model uncertainties, and smaller fin angle input than the existing pitch-and-depth loop PD depth controller.

1. Introduction

Autonomous underwater vehicles (AUVs) provide a safe, efficient, and economical way for amount of deep oceanic missions in comparison with those having human involved, in which the potential risk and operational cost could be prohibitively high (Shen et al., 2017). These missions include environmental monitoring, underwater inspection of estuaries and harbors, pipeline inspection, oceanographic and biological surveys, marine habitat mapping, offshore oil and gas exploration and exploitation, and obviating torpedoes, etc. (Moreira and Soares, 2008; Zhou et al., 2011; Santhakumar and Asokan, 2013; Shojaei and Arefi, 2015; Xiang et al., 2015; Yan et al., 2015; Zhang et al., 2015; Wang et al., 2016; Li and Yan, 2017; Qiao and Zhang, 2017, 2018a, 2018b; Qiao et al., 2017). For an underwater vehicle to be truly autonomous, it is necessary that it can be adaptive to the changing operating conditions, has the ability to reject the external disturbances and can effectively complete its preprogrammed tasks, without any kind of manual intervention. To meet the aforementioned requirements, the main task is to design a robust and efficient controller which can compensate for the hydrodynamic parametric uncertainties that affect the vehicle dynamic behaviour, copes with the external disturbances, guarantees the stability of the AUV system under all operating conditions, as well as provides good control performance.

The six degrees of freedom differential equations of motion of the AUV are commonly used to analyze the motion behaviour of the vehicle. This model is highly nonlinear and strongly coupled. For the convenience of use to design the controller in practice, it can be divided into three noninteracting or lightly interacting subsystems for speed control, steering, and diving (Jalving, 1994). This decomposition leads to a set of separate designs for speed, steering, and diving control systems. In Jalving (1994), separate PID controllers are designed for the decoupling speed, steering, and diving subsystems. In Prestero (2001), a simple inner-and-outer (pitch-and-depth) loop PD depth controller is developed for the diving subsystem. This paper devotes to the control strategy design for the diving subsystem as in Prestero (2001).

The use of optimal control theory to give a systematic procedure for the design of feedback control systems is one of the key ideas in the field of modern control (Petersen et al., 2000). Two typical optimization criterions are the 2 and infinity norms of the system. The H_∞ optimal control problem aims at minimizing the infinity norm of the system, that is, it reduces the maximum disturbance affecting the system. H_∞ controllers design for AUVs can refer to Campa et al. (1998), Feng and Allen (2004), Silvestre and Pascoal (2007), Moreira and Soares (2008), Cutipa-Luque and Donha (2011), Nag et al. (2013), and Zhang et al. (2016, 2017). The H_2 optimal control problem is the linear quadratic Gaussian (LQG) problem formulated as a system 2-

* Corresponding author.
E-mail addresses: qiaolei2008114106@gmail.com (L. Qiao), shitaoruan@gmail.com (S. Ruan), zgq_dlmu@163.com (G. Zhang), wdzhang@sjtu.edu.cn (W. Zhang).

https://doi.org/10.1016/j.oceaneng.2018.07.019
Received 19 April 2017; Received in revised form 25 May 2018; Accepted 8 July 2018
Available online 11 July 2018
0029-8018/

norm optimization problem. Formulating LQG as H_2 optimization is useful since it can be generalized to include frequency-domain performance specifications. The H_2 optimal control problem is to find out the linear, time invariant controller for the plant that stabilizes the closed-loop system and minimizes the system 2-norm. It provides a useful technique for the design of multivariable output feedback controllers and allows the designer to deal with robustness issues in a systematic manner. The H_2 optimal control methodology has been applied to underwater vehicles in Milliken (1984), Moreira and Soares (2008), Fossen (2011), and Wadoo et al. (2012) and to surface vehicles in Majohr and Buch (2006) and Wang et al. (2014). However, the aforementioned H_∞ and H_2 control methods for AUVs are not designed specifically for the problem of the input delay. In practical applications, the input delay often appears in the AUV control system. Such kind of time delay may affect the stability and performance of the control system. Thus, the design of the control method which can effectively deal with the input delay in the AUV control system is of practical importance.

Based on Zhang (2011), a robust H_2 optimal control strategy is proposed to deal with the problem of the depth-plane motion control of an AUV with output disturbances and time delay. The kinematics and dynamics of the AUV are firstly introduced through six degrees of freedom differential equations of motion using inertial and body-fixed reference frames. Because of the hydrodynamic force effects, the equations of motion of the vehicle are highly nonlinear and strongly coupled. From the practical point of view, it is essential to consider a linear and reduced-order model for efficient controller design. Therefore, the depth-plane dynamics of the AUV are then linearized and a linear and reduced-order model is obtained. By utilizing this linearized and reduced-order model, a robust H_2 optimal control method is developed, which takes into account both the output disturbances and time delay. Considering that the model of the AUV is uncertain due to the varying environmental conditions, thereby the robust stability and robust performance of the proposed control method are investigated. Simulation results show that the proposed robust H_2 optimal control strategy has good performance and holds many advantages comparing to the pitch-and-depth loop PD depth controller (Prestero, 2001) including higher tracking accuracy, better output disturbances rejection ability, stronger robustness against model uncertainties, and smaller fin angle input.

The structure of this paper is as follows. The AUV modeling including the six degrees of freedom nonlinear kinematic and dynamic models and the linearized depth-plane model is described in Section 2. In Section 3, a robust H_2 optimal control strategy is proposed for the depth-plane motion of the AUV in the presence of output disturbances and time delay, and the robust stability and robust performance of the proposed control method under model uncertainties are also discussed. In Section 4, the simulation results and comparisons with the existing pitch-and-depth loop PD depth controller are presented. Finally, conclusions are drawn in Section 5.

2. AUV modeling

The vehicle considered in this study is the REMUS AUV (Fig. 1) developed by von Alt and associates at the Woods Hole Oceanographic Institute's Oceanographic System Laboratory (WHOI OSL) (von Alt and Grassle, 1992). The REMUS is a small, low-cost AUV used for autonomous docking, long-range oceanographic survey, and shallow-water mine reconnaissance (von Alt et al., 1994). It is equipped with four identical control fins, mounted in a cruciform pattern near the aft end of the hull. The equations of motion of the REMUS AUV are given as follows.

2.1. Nonlinear model of the REMUS AUV

The notations used in this paper are in accordance with SNAME

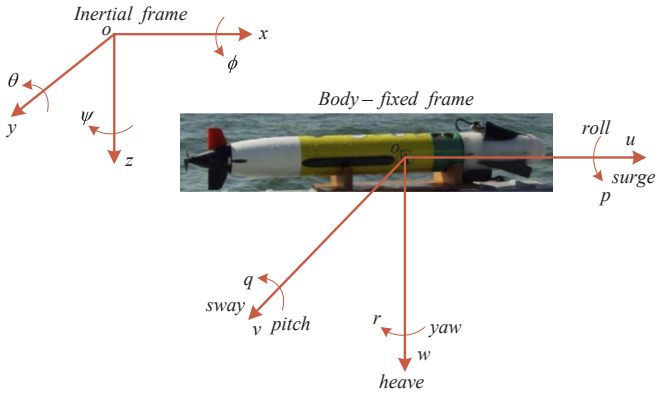

Fig. 1. AUV coordinate systems.

(SNAME, 1950). To determine the six degrees of freedom nonlinear equations of motion of the AUV, two reference frames are generally considered: one is the inertial or the earth-fixed frame which is considered to be stationary and the other is the body-fixed frame which is assumed to be fixed to the body of the vehicle and moves along with it. The diagram of the vehicle coordinate systems is shown in Fig. 1. The inertial and the body-fixed frames are represented by two vectors η and υ, respectively, where $\eta = [x,\ y,\ z,\ \phi,\ \theta,\ \psi]^T$ is the position and attitude vector of the vehicle with respect to the inertial frame, $x, y, z \in R$ are the position coordinates, $\phi, \theta, \psi \in R$ are the attitude coordinates (roll, pitch, and yaw), $\upsilon = [u,\ v,\ w,\ p,\ q,\ r]^T$ is the linear and angular velocities vector of the vehicle with respect to the body-fixed frame, $u, v, w \in R$ are the surge, sway, and heave velocities, $p, q, r \in R$ are the corresponding angular velocities. Through the coordinate frame transition, the kinematics of the REMUS AUV are described as (Prestero, 2001)

$$\begin{bmatrix}\dot{x}\\ \dot{y}\\ \dot{z}\end{bmatrix} = \underbrace{\begin{bmatrix} c\psi c\theta & -s\psi c\phi + c\psi s\theta s\phi & s\psi s\phi + c\psi s\theta c\phi \\ s\psi c\theta & c\psi c\phi + s\psi s\theta s\phi & -c\psi s\phi + s\psi s\theta c\phi \\ -s\theta & c\theta s\phi & c\theta c\phi \end{bmatrix}}_{J_1(\eta)} \begin{bmatrix} u\\ v\\ w\end{bmatrix} \tag{1}$$

$$\begin{bmatrix}\dot{\phi}\\ \dot{\theta}\\ \dot{\psi}\end{bmatrix} = \underbrace{\begin{bmatrix} 1 & s\phi t\theta & c\phi t\theta \\ 0 & c\phi & -s\phi \\ 0 & s\phi/c\theta & c\phi/c\theta \end{bmatrix}}_{J_2(\eta)} \begin{bmatrix} p\\ q\\ r\end{bmatrix} \tag{2}$$

in which $s\cdot$, $c\cdot$, and $t\cdot$ denote $\sin(\cdot)$, $\cos(\cdot)$, and $\tan(\cdot)$, respectively.

Remark 1. Note that $J_2(\eta)$ is not defined for pitch angle $\theta = \pm 90°$. However, as reported in Do and Pan (2009), AUVs are not likely to enter the neighbourhood of $\theta = \pm 90°$ because of the metacentric restoring forces. Thus, the singularity of $J_2(\eta)$ is not ordinarily approached.

Given that the body-fixed frame is centered at the vehicle center of buoyancy, the six degrees of freedom nonlinear dynamic equations of motion of the REMUS AUV are given by (Prestero, 2001).

Surge, or translation along the x-axis:

$$\begin{aligned}&(m - X_{\dot{u}})\dot{u} + mz_g\dot{q} - my_g\dot{r} = -(W - B)\sin\theta + X_{u|u|}u|u| \\ &+ (X_{wq} - m)wq + (X_{qq} + mx_g)q^2 \\ &+ (X_{vr} + m)vr + (X_{rr} + mx_g)r^2 \\ &- my_gpq - mz_gpr + X_{prop}\end{aligned} \tag{3a}$$

Sway, or translation along the y-axis:

$$(m - Y_{\dot{v}})\dot{v} + mz_g\dot{p} + (mx_g - Y_{\dot{r}})\dot{r} = (W - B)\cos\theta\sin\phi$$

$$+ Y_{v|v|}v|v| + Y_{r|r|}r|r| + my_g r^2$$

$$+ (Y_{ur} - m)ur + (Y_{wp} + m)wp$$

$$+ (Y_{pq} - mx_g)pq + Y_{uv}uv + my_g p^2$$

$$+ mz_g qr + Y_{uu\delta_r}u^2\delta_r \tag{3b}$$

Heave, or translation along the z-axis:

$$(m - Z_{\dot{w}})\dot{w} + my_g\dot{p} - (mx_g + Z_{\dot{q}})\dot{q} = (W - B)\cos\theta\cos\phi$$

$$+ Z_{w|w|}w|w| + Z_{q|q|}q|q|$$

$$+ (Z_{uq} + m)uq + (Z_{vp} - m)vp$$

$$+ (Z_{rp} - mx_g)rp + Z_{uw}uw + mz_g(p^2 + q^2)$$

$$- my_g rq + Z_{uu\delta_s}u^2\delta_s \tag{3c}$$

Roll, or rotation along the x-axis:

$$- mz_g\dot{v} + my_g\dot{w} + (I_{xx} - K_{\dot{p}})\dot{p} = -y_g W\cos\theta\cos\phi$$

$$- z_g W\cos\theta\sin\phi + K_{p|p|}p|p| - (I_{zz} - I_{yy})qr$$

$$+ m(uq - vp) - mz_g(wp - ur) + K_{prop} \tag{3d}$$

Pitch, or rotation along the y-axis:

$$mz_g\dot{u} - (mx_g + M_{\dot{w}})\dot{w} + (I_{yy} - M_{\dot{q}})\dot{q} = -z_g W\sin\theta$$

$$- x_g W\cos\theta\cos\phi + M_{w|w|}w|w| + M_{q|q|}q|q|$$

$$+ (M_{uq} - mx_g)uq + (M_{vp} + mx_g)vp$$

$$+ [M_{rp} - (I_{xx} - I_{zz})]rp + mz_g(vr - wq)$$

$$+ M_{uw}uw + M_{uu\delta_s}u^2\delta_s \tag{3e}$$

Yaw, or rotation along the z-axis:

$$- my_g\dot{u} + (mx_g - N_{\dot{v}})\dot{v} + (I_{zz} - N_{\dot{r}})\dot{r} = -x_g W\cos\theta\sin\phi$$

$$- y_g W\sin\theta + N_{v|v|}v|v| + N_{r|r|}r|r|$$

$$+ (N_{ur} - mx_g)ur + (N_{wp} + mx_g)wp$$

$$+ [N_{pq} - (I_{yy} - I_{xx})]pq - my_g(vr - wq)$$

$$+ N_{uv}uv + M_{uu\delta_r}u^2\delta_r. \tag{3f}$$

In (3a)-(3f), m is the vehicle mass, $W = mg$ is the vehicle weight, $B = \rho\nabla g$ is the vehicle buoyancy where ρ is the density of the surrounding fluid and ∇ is the total volume displaced by the vehicle, (x_g, y_g, z_g) are the coordinates of the vehicle center of gravity in the body-fixed frame, I_{xx}, I_{yy}, I_{zz} are the moments of inertia about x, y, z axis, respectively, $X_{\dot{u}}$, X_{wq}, X_{qq}, X_{vr}, X_{rr}, $Y_{\dot{v}}$, $Y_{\dot{r}}$, Y_{ur}, Y_{wp}, Y_{pq}, $Z_{\dot{w}}$, $Z_{\dot{q}}$, Z_{uq}, Z_{vp}, Z_{rp}, $K_{\dot{p}}$, $M_{\dot{w}}$, $M_{\dot{q}}$, M_{uq}, M_{vp}, M_{rp}, $N_{\dot{v}}$, $N_{\dot{r}}$, N_{ur}, N_{wp}, N_{pq} are the added mass terms, $X_{u|u|}$, $Y_{v|v|}$, $Y_{r|r|}$, $Z_{w|w|}$, $Z_{q|q|}$, $M_{w|w|}$, $M_{q|q|}$, $N_{v|v|}$, $N_{r|r|}$ are the cross-flow drag terms, X_{prop} and K_{prop} are the propeller thrust and torque, respectively, Y_{uv} and Z_{uw} are the body lift force and fin lift terms, M_{uw} and N_{uv} are the body and fin lift and Munk moment terms, $Y_{uu\delta_r}$ and $Z_{uu\delta_s}$ are the fin lift force terms, $M_{uu\delta_s}$ and $M_{uu\delta_r}$ are the fin lift moment terms, $K_{p|p|}$ is the rolling resistance, and δ_r and δ_s are the fin angles.

Remark 2. Note that the vehicle cross-products of inertia, I_{xy}, I_{xz}, and I_{yz} are assumed to be small and are neglected in the above dynamic equations of motion. Similarly, the equations do not include zero-valued coefficients (Prestero, 2001).

2.2. Linearized depth-plane model of the REMUS AUV

The above vehicle model is highly nonlinear and strongly coupled. From the practical point of view, it is essential to consider a linear and reduced-order model for efficient controller design. Therefore, the decomposition of the whole AUV system into speed, steering, and diving subsystems as presented in Jalving (1994) is chosen. In this paper we only consider the diving motion of the AUV. Assuming that z_g is small, the simplified vehicle depth-plane dynamics are given by (Prestero, 2001)

$$(m - Z_{\dot{w}})\dot{w} - (mx_g + Z_{\dot{q}})\dot{q} - Z_w w - (mU + Z_q)q = Z_{\delta_s}\delta_s \tag{4a}$$

$$- (mx_g + M_{\dot{w}})\dot{w} + (I_{yy} - M_{\dot{q}})\dot{q} - M_w w + (mx_g U - M_q)q - M_\theta\theta = M_{\delta_s}\delta_s \tag{4b}$$

where U is the steady-state forward velocity of the vehicle, Z_w, Z_q, M_w, M_q are the combined terms, M_θ is the hydrostatic term, and Z_{δ_s} and M_{δ_s} are the fin lift and moment coefficients, respectively. The reduced kinematic equations of motion are described as (Prestero, 2001)

$$\dot{z} = w - U\theta \tag{5a}$$

$$\dot{\theta} = q. \tag{5b}$$

Combining (4) and (5) allow us to obtain

$$\begin{bmatrix} m - X_{\dot{u}} & -(mx_g + Z_{\dot{q}}) & 0 & 0 \\ -(mx_g + M_{\dot{w}}) & I_{yy} - M_{\dot{q}} & 0 & 0 \\ 0 & 0 & 1 & 0 \\ 0 & 0 & 0 & 1 \end{bmatrix}\begin{bmatrix} \dot{w} \\ \dot{q} \\ \dot{z} \\ \dot{\theta} \end{bmatrix} - \begin{bmatrix} Z_w & mU + Z_q & 0 & 0 \\ M_w & -mx_g U + M_q & 0 & M_\theta \\ 1 & 0 & 0 & -U \\ 0 & 1 & 0 & 0 \end{bmatrix}\begin{bmatrix} w \\ q \\ z \\ \theta \end{bmatrix} = \begin{bmatrix} Z_{\delta_s} \\ M_{\delta_s} \\ 0 \\ 0 \end{bmatrix}\delta_s. \tag{6}$$

The heave velocity w during diving is usually small, so the above model can be further simplified to

$$\begin{bmatrix} I_{yy} - M_{\dot{q}} & 0 & 0 \\ 0 & 1 & 0 \\ 0 & 0 & 1 \end{bmatrix}\begin{bmatrix} \dot{q} \\ \dot{z} \\ \dot{\theta} \end{bmatrix} + \begin{bmatrix} -M_q & 0 & -M_\theta \\ 0 & 0 & U \\ -1 & 0 & 0 \end{bmatrix}\begin{bmatrix} q \\ z \\ \theta \end{bmatrix} = \begin{bmatrix} M_{\delta_s} \\ 0 \\ 0 \end{bmatrix}\delta_s. \tag{7}$$

Writing the above equation in state space form yields

$$\begin{bmatrix} \dot{q} \\ \dot{z} \\ \dot{\theta} \end{bmatrix} = \begin{bmatrix} \frac{M_q}{I_{yy} - M_{\dot{q}}} & 0 & \frac{M_\theta}{I_{yy} - M_{\dot{q}}} \\ 0 & 0 & -U \\ 1 & 0 & 0 \end{bmatrix}\begin{bmatrix} q \\ z \\ \theta \end{bmatrix} + \begin{bmatrix} \frac{M_{\delta_s}}{I_{yy} - M_{\dot{q}}} \\ 0 \\ 0 \end{bmatrix}\delta_s. \tag{8}$$

The model (8) is well suited for controller design. Now we will derive the vehicle transfer functions for the subsequent control strategy design. We first derive the transfer function for the inner pitch loop, relating input stern plane angle δ_s to the output pitch angle θ. By taking the Laplace transform of the state space equation (8), we can obtain the pitch open-loop transfer function $\theta(s)/\delta_s(s)$ as

$$\frac{\theta(s)}{\delta_s(s)} = \frac{\frac{M_{\delta_s}}{I_{yy} - M_{\dot{q}}}}{s^2 - \frac{M_q}{I_{yy} - M_{\dot{q}}}s - \frac{M_\theta}{I_{yy} - M_{\dot{q}}}} = \frac{k}{s^2 + 2\xi\varpi s + \varpi^2} \tag{9}$$

where the gain constant k is $k = M_{\delta_s}/(I_{yy} - M_{\dot{q}})$, and the natural frequency ϖ and the relative damping ratio ξ are

$$\varpi = \sqrt{\frac{-M_\theta}{I_{yy} - M_{\dot{q}}}}, \xi = \frac{-M_q}{2\sqrt{-M_\theta(I_{yy} - M_{\dot{q}})}}. \tag{10}$$

Next we will derive the transfer function for the outer depth loop, which relates the input pitch angle θ_d to the output depth z. In practice, the inner pitch loop responses are sufficiently fast enough in contrast to the outer depth loop. Therefore, we can consider the desired pitch angle θ_d to be the same as the actual pitch angle θ. In the same way, taking the Laplace transform of (8), we get the depth open-loop transfer functions as

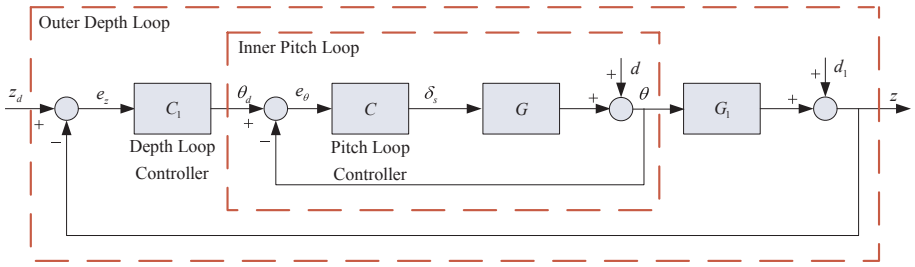

Fig. 2. Block diagram of the vehicle depth-plane control system.

$$\frac{z(s)}{\theta(s)} = -\frac{U}{s}. \tag{11}$$

Supposing that there exists input delay, then the open-loop transfer function of the pitch loop becomes

$$G(s) = \frac{\theta(s)}{\delta_s(s)}e^{-\tau s} = \frac{ke^{-\tau s}}{s^2 + 2\xi\varpi s + \varpi^2} \tag{12}$$

where τ is a positive real number denoting the time delay, and the open-loop transfer function of the depth loop is

$$G_1(s) = \frac{z(s)}{\theta(s)} = -\frac{U}{s}. \tag{13}$$

3. Robust H_2 optimal depth control strategy design

The vehicle depth-plane control system can be summarized as the following block diagram.

In Fig. 2, θ_d is the desired vehicle pitch angle, z_d is the desired vehicle depth, e_θ and e_z are the corresponding pitch angle and depth errors, respectively, d and d_1 are the output disturbances of the pitch and depth loops, respectively, C is the pitch loop controller, and C_1 is the depth loop controller.

The aim of this paper is to design the controllers C and C_1 for the inner pitch and outer depth loops, respectively, with the consideration of the output disturbances and time delay. The H_2 optimal control design methods proposed in Zhang (2011) will be used in the two controllers design.

The design of the robust H_2 optimal controllers C and C_1 are based on the internal model control (IMC) structure (Morari and Zafiriou, 1989). The IMC structure of the vehicle depth-plane control system is shown in Fig. 3, where $\tilde{G}$ is the pitch loop plant, G is the pitch loop model, Q is the design pitch loop transfer function, $\tilde{G}_2 = \tilde{G}_1\tilde{G}_0$ is the depth loop plant, $\tilde{G}_0$ is the real closed-loop transfer function of the pitch loop, $\tilde{G}_1$ is the real open-loop transfer function of the depth loop, $G_2 = G_1G_0$ is the depth loop model, G_0 is the nominal closed-loop transfer function of the pitch loop, G_1 is the nominal open-loop transfer function of the depth loop, and Q_1 is the design depth loop transfer function.

Assuming that the depth-plane model is exact, the sensitivity transfer function and the complementary transfer function for the pitch loop are given by

$$S(s) = \frac{1}{1 + G(s)C(s)} \tag{14a}$$

$$T(s) = \frac{G(s)C(s)}{1 + G(s)C(s)} \tag{14b}$$

and the sensitivity transfer function and the complementary transfer function for the depth loop are given by

$$S_1(s) = \frac{1}{1 + G_2(s)C_1(s)} \tag{15a}$$

$$T_1(s) = \frac{G_2(s)C_1(s)}{1 + G_2(s)C_1(s)}. \tag{15b}$$

Defining the transfer functions Q and Q_1 as

$$Q(s) = \frac{C(s)}{1 + G(s)C(s)} \tag{16}$$

$$Q_1(s) = \frac{C_1(s)}{1 + G_2(s)C_1(s)} \tag{17}$$

it follows that

$$S(s) = 1 - G(s)Q(s) \tag{18a}$$

$$T(s) = G(s)Q(s) \tag{18b}$$

and

$$S_1(s) = 1 - G_2(s)Q_1(s) \tag{19a}$$

$$T_1(s) = G_2(s)Q_1(s). \tag{19b}$$

From (16) and (17), the IMC based controllers C and C_1 are given by

$$C(s) = \frac{Q(s)}{1 - G(s)Q(s)} \tag{20}$$

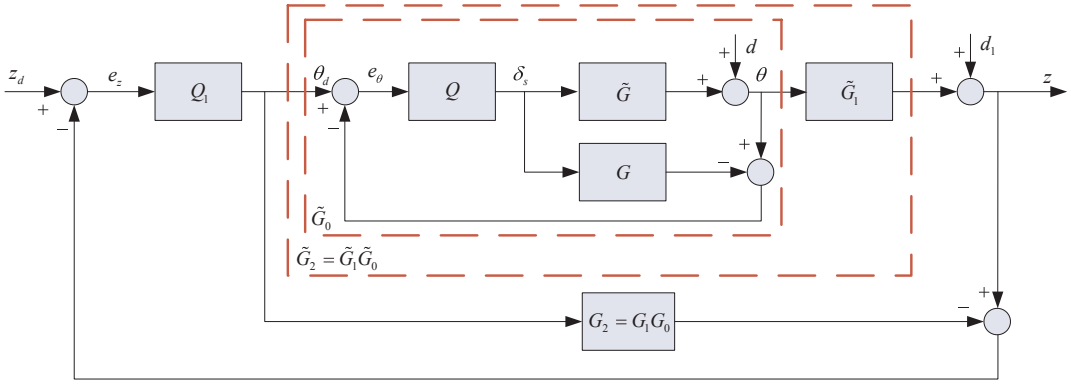

Fig. 3. IMC structure of the vehicle depth-plane control system.

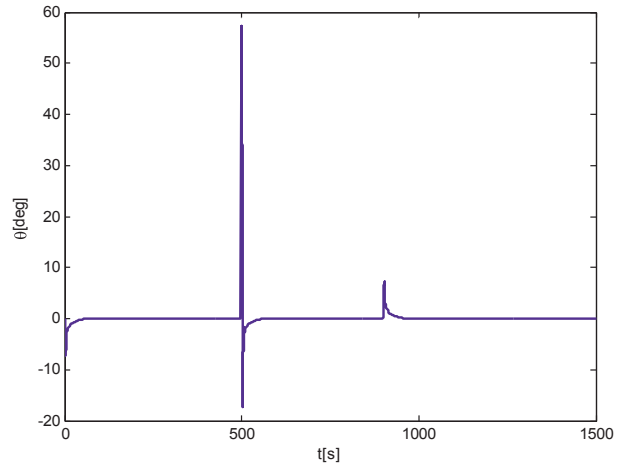

(a) Pitch angle for robust H_2 optimal control strategy.

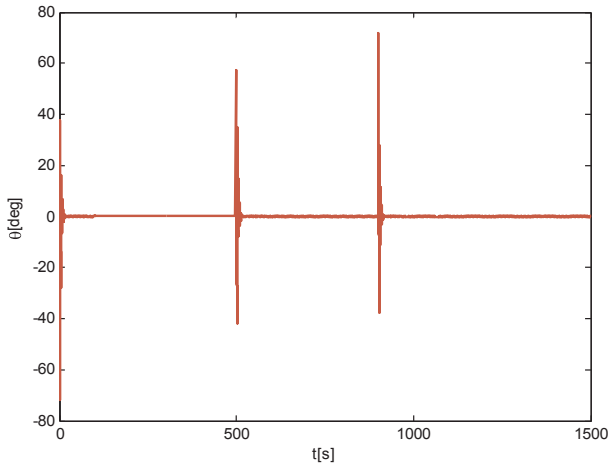

(b) Pitch angle for the controller proposed in Prestero (2001).

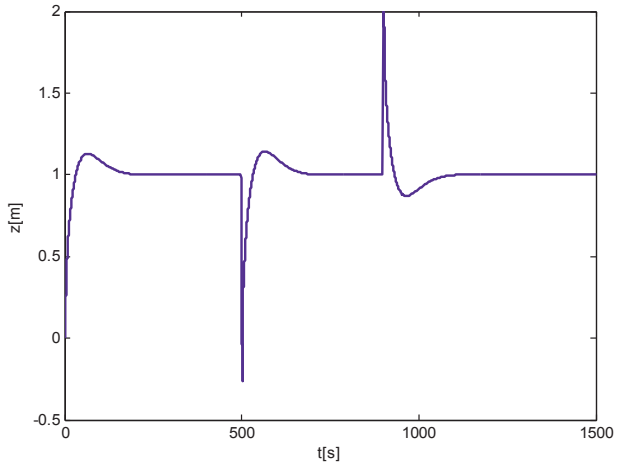

(c) Depth for robust H_2 optimal control strategy.

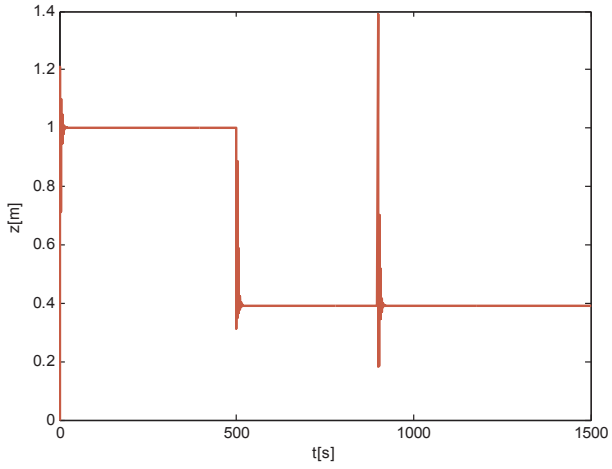

(d) Depth for the controller proposed in Prestero (2001).

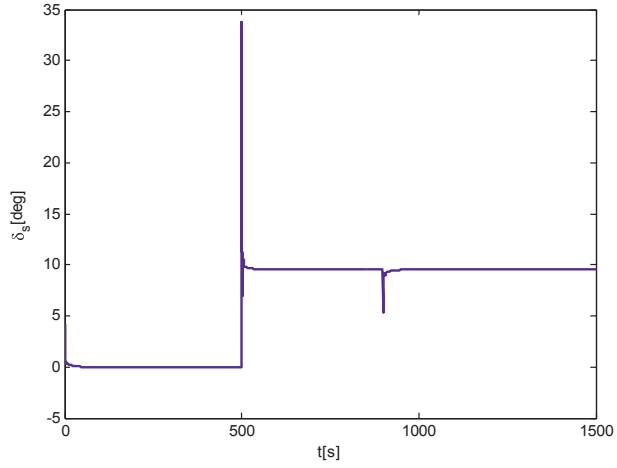

(e) Fin angle for robust H_2 optimal control strategy.

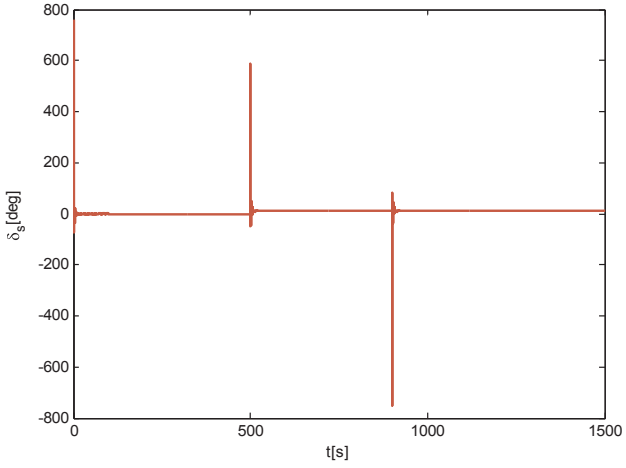

(f) Fin angle for the controller proposed in Prestero (2001).

Fig. 4. Step responses of the nominal vehicle dynamic model with robust H_2 optimal control strategy and the controller proposed in Prestero (2001).

$$C_1(s) = \frac{Q_1(s)}{1 - G_2(s)Q_1(s)}. \tag{21}$$

The following lemma is essential to derive the proposed robust H_2 optimal pitch and depth loop controllers C and C_1.

Lemma 1. (Zhou, 1998). *Introduce the symbol L_2 for the family of all strictly proper functions with no poles on the imaginary axis. Let H_2 denote*

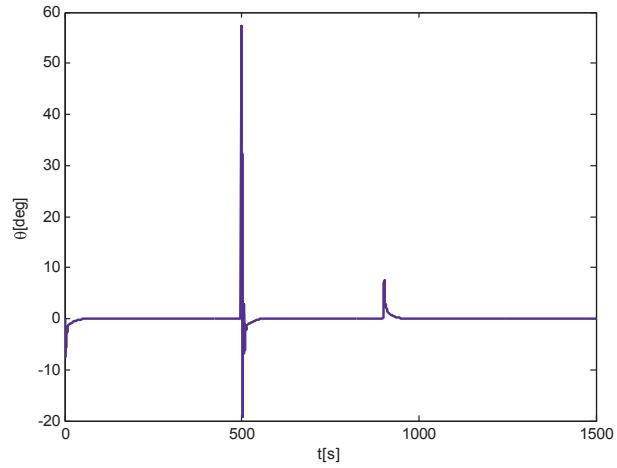

(a) Pitch angle for robust H_2 optimal control strategy.

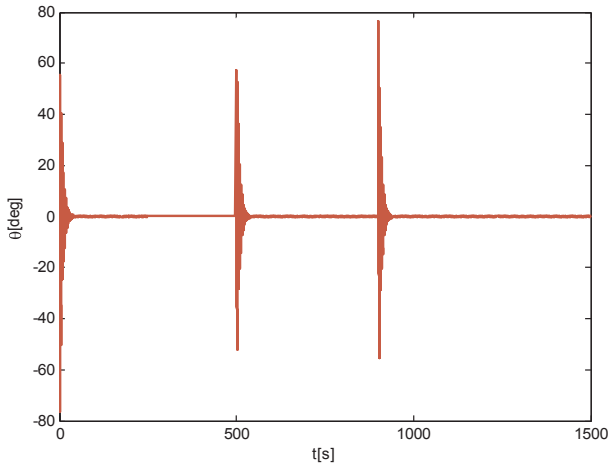

(b) Pitch angle for the controller proposed in Prestero (2001).

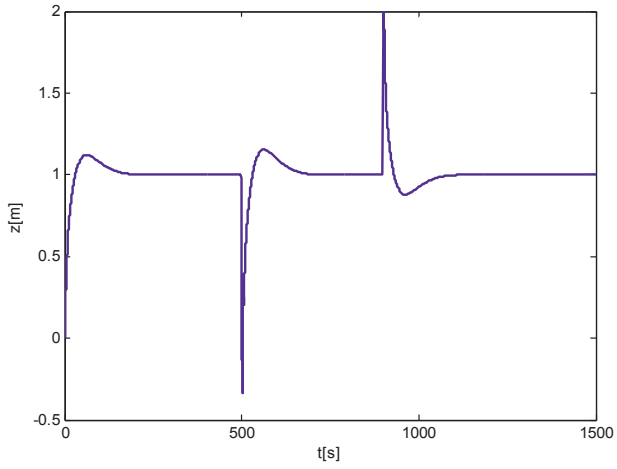

(c) Depth for robust H_2 optimal control strategy.

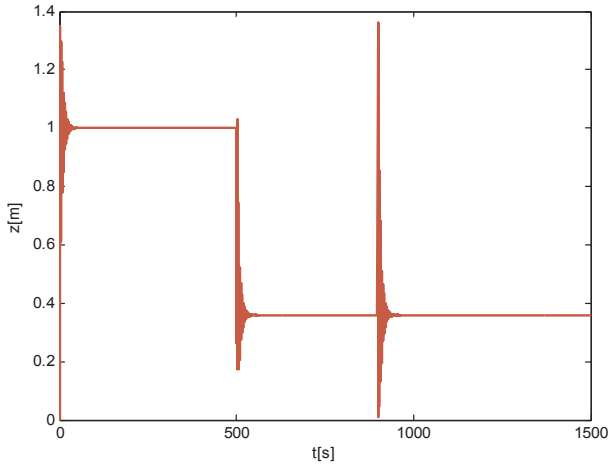

(d) Depth for the controller proposed in Prestero (2001).

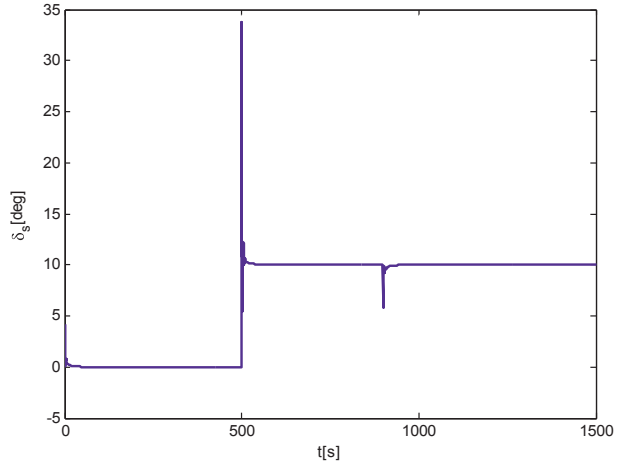

(e) Fin angle for robust H_2 optimal control strategy.

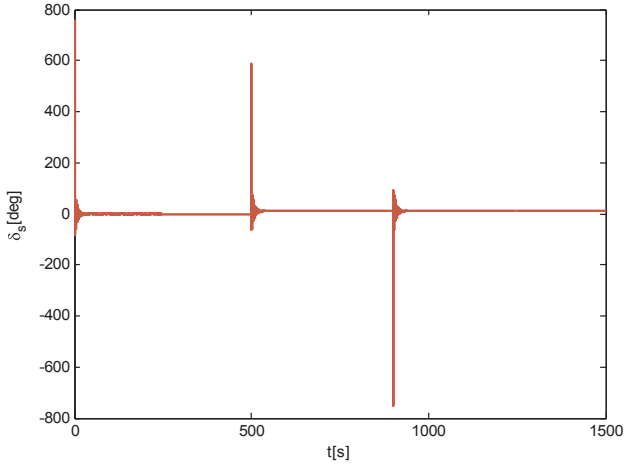

(f) Fin angle for the controller proposed in Prestero (2001).

Fig. 5. Step responses of the uncertain vehicle dynamic model with robust H_2 optimal control strategy and the controller proposed in Prestero (2001).

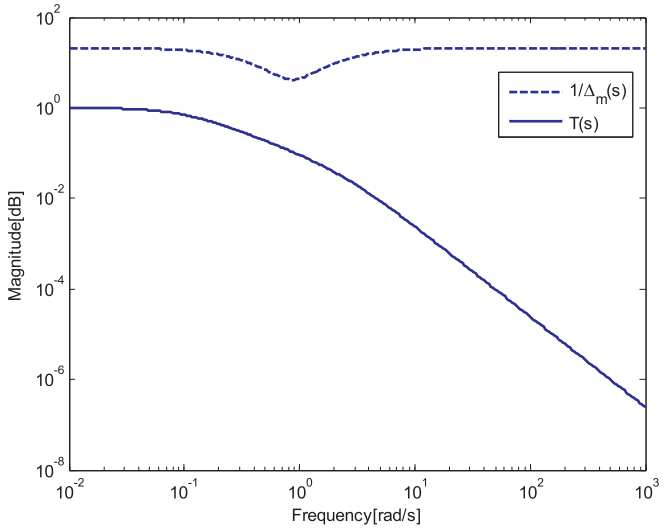

(a) Magnitudes of $1/\Delta_m(s)$ and T(s) for pitch loop.

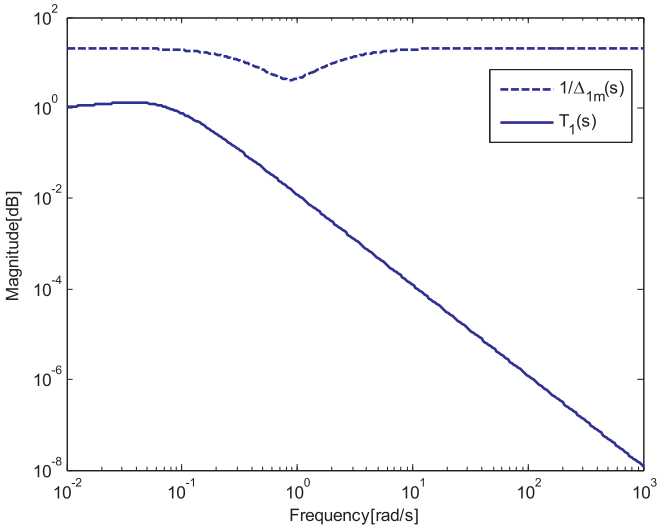

(b) Magnitudes of $1/\Delta_{1m}(s)$ and $T_1(s)$ for depth loop.

Fig. 6. Verification of the robust stability of pitch and depth loops with robust H_2 optimal control strategy.

the subset of L_2 *and analytic in* Res>0, $H_2^{\perp}$ *analytic in* Res ≤ 0, *and* $H_2 + H_2^{\perp}$ *the set of all sums. Every function* $F(s)$ *in* L_2 *can be uniquely expressed as* $F = F_1 + F_2$, $F_1 \in H_2$, $F_2 \in H_2^{\perp}$. *Then*

$$\|F_1 + F_2\|_2^2 = \|F_1\|_2^2 + \|F_2\|_2^2. \tag{22}$$

3.1. Robust H_2 optimal pitch loop controller design

$G(s)$ given in equation (12) can be rewritten in the following form

$$G(s) = \frac{Ke^{-\tau s}}{(\tau_1 s + 1)(\tau_2 s + 1)} \tag{23}$$

where $K = \frac{k}{\varpi^2}$, $\tau_1 = \frac{\xi}{\varpi} - \frac{1}{\varpi}\sqrt{\xi^2 - 1}$, and $\tau_2 = \frac{\xi}{\varpi} + \frac{1}{\varpi}\sqrt{\xi^2 - 1}$.

Remark 3. According to the hydrodynamic coefficients of the REMUS AUV given in Prestero (2001), we obtain that $\mathrm{Res}(\tau_1) > 0$ and $\mathrm{Res}(\tau_2) > 0$. Thus $G(s)$ is stable. The details can be seen in Section 4.

By using the first-order Taylor expansion of $e^{-\tau s}$, we obtain

$$G(s) \approx \frac{K(1 - \tau s)}{(\tau_1 s + 1)(\tau_2 s + 1)}. \tag{24}$$

The H_2 optimal index is chosen as

$$\min \|W(s)S(s)\|_2 \tag{25}$$

where $W(s)$ is the weighting function. Although the following design procedure is sufficiently general for ramp or more complex inputs, we consider only step input for clarity. Hence, $W(s) = 1/s$.

Remark 4. Normally, there are abundant sinusoidal signals whose amplitudes decrease with frequencies in a step signal. Therefore, the step signal is a reasonable and sufficiently strict choice for system analysis.

According to Zhang (2011), to guarantee internal stability and the asymptotic property of the closed-loop system, $Q(s)$ should be stable and the following constraint condition should be met

$$\lim_{s\to 0} S(s) = \lim_{s\to 0}[1 - G(s)Q(s)] = 0. \tag{26}$$

(26) gives

$$Q(0) = \frac{1}{G(0)} = \frac{1}{K}. \tag{27}$$

The set of all the stable transfer functions $Q(s)$ satisfying the above constraint condition can be written as

$$Q(s) = \frac{1}{K} + sQ'(s) \tag{28}$$

where $Q'(s)$ is stable.

Therefore, the function to be minimized can be written as

$$\begin{aligned}
&\|W(s)S(s)\|_2^2 \\
&= \left\| \frac{1}{s}\left\{1 - G(s)\left[\frac{1}{K} + sQ'(s)\right]\right\}\right\|_2^2 \\
&= \left\| \frac{\tau_1\tau_2 s + \tau_1 + \tau_2 + \tau}{(\tau_1 s + 1)(\tau_2 s + 1)} - \frac{K(1 - \tau s)Q'(s)}{(\tau_1 s + 1)(\tau_2 s + 1)}\right\|_2^2 \\
&= \left\| \frac{1 - \tau s}{1 + \tau s}\left[\frac{(\tau_1\tau_2 s + \tau_1 + \tau_2 + \tau)(1 + \tau s)}{(\tau_1 s + 1)(\tau_2 s + 1)(1 - \tau s)} - \frac{K(1 + \tau s)Q'(s)}{(\tau_1 s + 1)(\tau_2 s + 1)}\right]\right\|_2^2.
\end{aligned} \tag{29}$$

Since $(1 - \tau s)/(1 + \tau s)$ is an all-pass transfer function. By the definition of 2-norm, it is easy to verify that the 2-norm of a transfer function keeps its value after an all-pass transfer function is introduced to it. Thus, we have

$$\begin{aligned}
&\|W(s)S(s)\|_2^2 \\
&= \left\| \frac{(\tau_1\tau_2 s + \tau_1 + \tau_2 + \tau)(1 + \tau s)}{(\tau_1 s + 1)(\tau_2 s + 1)(1 - \tau s)} - \frac{K(1 + \tau s)Q'(s)}{(\tau_1 s + 1)(\tau_2 s + 1)}\right\|_2^2 \\
&= \left\| \frac{2\tau}{1 - \tau s} + \frac{\tau_1\tau_2 s + \tau_1 + \tau_2 - \tau}{(\tau_1 s + 1)(\tau_2 s + 1)} - \frac{K(1 + \tau s)Q'(s)}{(\tau_1 s + 1)(\tau_2 s + 1)}\right\|_2^2.
\end{aligned} \tag{30}$$

According to Lemma 1, we have

$$\|W(s)S(s)\|_2^2 = \left\| \frac{2\tau}{1 - \tau s}\right\|_2^2 + \left\| \frac{\tau_1\tau_2 s + \tau_1 + \tau_2 - \tau}{(\tau_1 s + 1)(\tau_2 s + 1)} - \frac{K(1 + \tau s)Q'(s)}{(\tau_1 s + 1)(\tau_2 s + 1)}\right\|_2^2. \tag{31}$$

Temporarily relax the requirement on the properness of $Q(s)$. To minimize the right-hand side of (31), the only choice is

$$Q'_{opt}(s) = \frac{\tau_1\tau_2 s + \tau_1 + \tau_2 - \tau}{K(1 + \tau s)}. \tag{32}$$

Substituting (32) into (28) yields the optimal $Q(s)$ as

$$Q_{opt}(s) = \frac{1}{K} + sQ'_{opt}(s)$$

$$= \frac{(\tau_1 s + 1)(\tau_2 s + 1)}{K(1 + \tau s)}. \tag{33}$$

Note that $Q_{opt}(s)$ is improper due to that the order of its numerator is greater than the order of its denominator. To make it proper, a filter for which numerator order is less than the denominator order should be introduced. Meanwhile, the filter should ensure the internal stability and the asymptotic property of the closed-loop system, i.e., $Q_{opt}(s)J(s)$ is stable and

$$\lim_{s\to 0}[1 - G(s)Q_{opt}(s)J(s)] = 0. \tag{34}$$

With this in mind, we choose the following filter

$$J(s) = \frac{1}{\lambda s + 1} \tag{35}$$

where λ is the performance degree and it is a positive real number.

Thus, the suboptimal $Q(s)$ after introducing the filter is

$$Q(s) = Q_{opt}(s)J(s)$$

$$= \frac{(\tau_1 s + 1)(\tau_2 s + 1)}{K(1 + \tau s)(\lambda s + 1)}. \tag{36}$$

From (20), the controller that makes the unity feedback pitch loop control system internally stable and has a zero steady-state error for a step reference can be obtained as

$$C(s) = \frac{Q(s)}{1 - G(s)Q(s)}$$

$$= \frac{1}{K}\frac{(\tau_1 s + 1)(\tau_2 s + 1)}{\lambda\tau s^2 + (\lambda + 2\tau)s}. \tag{37}$$

3.2. Robust H_2 optimal depth loop controller design

$G_2(s)$ in Fig. 3 can be written in the following form

$$G_2(s) = G_1(s)G_0(s) = G_1(s)G(s)Q(s)$$

$$= -\frac{U}{s}\frac{(1 - \tau s)}{(\lambda s + 1)(\tau s + 1)}$$

$$= \frac{K'(1 - \tau s)}{s(\lambda s + 1)(\tau s + 1)} \tag{38}$$

where $K' = -U$, and λ and τ are all positive real numbers that defined above.

The H_2 optimal index is chosen as

$$\min \|W_1(s)S_1(s)\|_2 \tag{39}$$

where $W_1(s)$ is the weighting function. Like in Section 3.1, here we also consider the step input for clarity. Thus, $W_1(s) = 1/s$.

According to Zhang (2011), to guarantee the internal stability of the closed-loop system, $Q_1(s)$ should be stable and the following constraint condition should be met

$$\lim_{s\to 0}[1 - G_2(s)Q_1(s)] = 0. \tag{40}$$

The set of all the stable transfer functions $Q_1(s)$ satisfying the above constraint condition can be expressed as

$$Q_1(s) = \frac{s[1 + sQ'_1(s)]}{K'} \tag{41}$$

where $Q'_1(s)$ is stable. This leads to

$$\|W_1(s)S_1(s)\|_2^2$$

$$= \left\| \frac{1}{s}\left\{1 - \frac{(1 - \tau s)[1 + sQ'_1(s)]}{(\lambda s + 1)(\tau s + 1)}\right\} \right\|_2^2$$

$$= \left\| \frac{\lambda\tau s + \lambda + 2\tau}{(\lambda s + 1)(\tau s + 1)} - \frac{(1 - \tau s)Q'_1(s)}{(\lambda s + 1)(\tau s + 1)} \right\|_2^2$$

$$= \left\| \frac{1 - \tau s}{1 + \tau s}\left[\frac{\lambda\tau s + \lambda + 2\tau}{(\lambda s + 1)(1 - \tau s)} - \frac{Q'_1(s)}{(\lambda s + 1)} \right] \right\|_2^2. \tag{42}$$

Since $(1 - \tau s)/(1 + \tau s)$ is an all-pass transfer function, we can obtain that

$$\|W_1(s)S_1(s)\|_2^2$$

$$= \left\| \frac{\lambda\tau s + \lambda + 2\tau}{(\lambda s + 1)(1 - \tau s)} - \frac{Q'_1(s)}{(\lambda s + 1)} \right\|_2^2$$

$$= \left\| \frac{2\tau}{1 - \tau s} + \frac{\lambda}{\lambda s + 1} - \frac{Q'_1(s)}{\lambda s + 1} \right\|_2^2. \tag{43}$$

From Lemma 1, we have

$$\|W_1(s)S_1(s)\|_2^2 = \left\| \frac{2\tau}{1 - \tau s} \right\|_2^2 + \left\| \frac{\lambda}{\lambda s + 1} - \frac{Q'_1(s)}{\lambda s + 1} \right\|_2^2. \tag{44}$$

Evidently, $Q'_{1opt}(s) = \lambda$ gives the optimal solution, which implies

$$Q_{1opt}(s) = \frac{s[1 + sQ'_{1opt}(s)]}{K'} = \frac{s(1 + \lambda s)}{K'}. \tag{45}$$

A filter should be introduced to make $Q_{1opt}(s)$ proper. Meanwhile, the filter should satisfy the constraints of the internal stability and the asymptotic property of the closed-loop system. However, since $G_2(s)$ contains an integrator, the constraints of the asymptotic property will be different from those in the pitch closed-loop system. According to Zhang (2011), here the constraints of the internal stability and the asymptotic property that the filter should meet are that $Q_{1opt}(s)J_1(s)$ is stable and

$$\lim_{s\to 0}[1 - G_2(s)Q_{1opt}(s)J_1(s)] = 0 \tag{46a}$$

$$\lim_{s\to 0}\frac{d}{ds}[1 - G_2(s)Q_{1opt}(s)J_1(s)] = 0. \tag{46b}$$

Taking these into account, the following filter is introduced

$$J_1(s) = \frac{(3\bar{\lambda} + 2\tau)s + 1}{(\bar{\lambda}s + 1)^3} \tag{47}$$

where $\bar{\lambda}$ is the performance degree and it is a positive real number.

Therefore, the suboptimal $Q_1(s)$ is

$$Q_1(s) = Q_{1opt}(s)J_1(s)$$

$$= \frac{1}{K'}\frac{s(\lambda s + 1)[(3\bar{\lambda} + 2\tau)s + 1]}{(\bar{\lambda}s + 1)^3}. \tag{48}$$

From (21), the unity feedback depth loop controller is obtained as

$$C_1(s) = \frac{Q_1(s)}{1 - G_2(s)Q_1(s)}$$

$$= \frac{1}{K'}\frac{(\lambda s + 1)(\tau s + 1)[(3\bar{\lambda} + 2\tau)s + 1]}{\bar{\lambda}^3\tau s^3 + (3\bar{\lambda}^2\tau + \bar{\lambda}^3)s^2 + (6\bar{\lambda}\tau + 3\bar{\lambda}^2 + 2\tau^2)s}. \tag{49}$$

Remark 5. In this paper, we only investigate the controllers design for the diving subsystem. However, the controllers design for the speed and steering subsystems can also use the same design methods.

3.3. Robust stability and robust performance discussion

In practical applications, uncertainties always exist in the AUV model. Assuming that the uncertainties in the pitch and depth loops are described by the multiplicative unstructured uncertainty $\Delta_m(s)$ and $\Delta_{1m}(s)$, respectively. That is, $\left|\frac{\tilde{G}(j\omega)-G(j\omega)}{G(j\omega)}\right| \le |\Delta_m(j\omega)|$ and $\left|\frac{\tilde{G}_2(j\omega)-G_2(j\omega)}{G_2(j\omega)}\right| \le |\Delta_{1m}(j\omega)|$. Then, according to Zhou (1998), for every frequency, the pitch closed-loop system is robust stable if and only if

$$\|T(s)\Delta_m(s)\|_\infty < 1 \tag{50}$$

and the depth closed-loop system is robust stable if and only if

$$\|T_1(s)\Delta_{1m}(s)\|_\infty < 1. \tag{51}$$

Although the robustness of the pitch and depth closed-loop systems can be rigorously calculated according to the aforementioned criterions, they are seldom adopted in practice, because of their complexity. There are usually strong constraints for the simplicity of tuning rules in practices.

The robust performance implies both robust stability and nominal performance. It is desirable to make $\|W(s)S(s)\|_\infty$ and $\|W_1(s)S_1(s)\|_\infty$ small for good nominal performance and at the same time make $\|T(s)\Delta_m(s)\|_\infty$ and $\|T_1(s)\Delta_{1m}(s)\|_\infty$ small for good robust stability. Unfortunately, the interdependence of $S(s)+T(s)=1$ and $S_1(s)+T_1(s)=1$ makes the objective a challenge. Improving the nominal performance worsens the robust stability and pushes the system close to instability. Conversely, good robust stability may be obtained by sacrificing the nominal performance. Therefore, how to reach a good tradeoff between nominal performance and robust stability is the main problem in control system design. For classical methods, it may be difficult to make a clear and reasonable tradeoff between nominal performance and robustness. Some new methods may be capable of making the tradeoff if the uncertainty profile is known. However, when the performance specification is changed or the uncertainty offsets, one must redesign the controller. The operator usually has no ability to redesign the controller. The designed robust H_2 optimal controllers are effective to tune the nominal performance and robustness quantitatively.

It can be verified that the larger the performance degrees λ and $\bar{\lambda}$, the better the robustness. But too large λ and $\bar{\lambda}$ will worsen the nominal performance. Based on the analysis, a simple and quantitative engineering tuning procedure developed by Zhang et al. (2006) is recommended here: increase λ and $\bar{\lambda}$ monotonically until the required pitch and depth loop responses are obtained. Normally, the step is 0.01τ.

Since λ and $\bar{\lambda}$ are directly related to the closed-loop responses of the pitch and depth loops, the operating personnel can use these two parameters as a knob. When the knowledge about the AUV model is rich (or the uncertainties reduce), a good nominal performance can be demanded by decreasing λ and $\bar{\lambda}$. When the knowledge about the AUV model is poor (or the uncertainties increase), a good robustness must be demanded by increasing λ and $\bar{\lambda}$.

Table 1
Hydrodynamic coefficients of the REMUS AUV.

Parameter	Value	Units	Description
I_{yy}	3.45	kgm^2	Moment of inertia along y axis
$M_{\dot{q}}$	−4.88	kgm^2	Added mass
M_q	−6.87	kgm^2/s	Combined term
M_θ	−5.77	kgm^2/s^2	Hydrostatic
M_{δ_s}	−34.6	kgm^2/s^2	Fin lift

4. Simulation results

Here some computer simulations are performed on the REMUS AUV to demonstrate the feasibility of the proposed control strategy. The linearized maneuvering nominal coefficient values of the REMUS AUV in depth plane are taken from Prestero (2001) and are listed in Table 1. Substituting the coefficient values in Table 1 into (9) and (10) we calculate that $k=-4.15$, $\varpi=0.83$, and $\xi=0.5$. Then, K, τ_1, and τ_2 can be calculated from (23) as $K=-6.02$, $\tau_1=0.602-1.04j$, and $\tau_2=0.602+1.04j$. Assuming that the input delay is $\tau=0.4s$ and substituting the above calculated parameter values into (23) and (37) we obtain the open-loop transfer function $G(s)$ of the pitch loop and the unity feedback pitch loop controller $C(s)$ as

$$G(s)=\frac{-4.15e^{-0.4s}}{s^2+0.83s+0.69} \tag{52}$$

$$C(s)=\frac{-1}{0.602}\frac{1.45s^2+1.2s+1}{0.4\lambda s^2+(\lambda+0.8)s}. \tag{53}$$

Usually the velocity of the underwater vehicles varies between $1m/s$ and $4m/s$. In this study, the velocity of the vehicle is considered to be $U=1m/s$ as in Nag et al. (2013). Thus, $K'=-U=-1$. Substituting the values of U, K', and τ into (13) and (49) results in the open-loop transfer function $G_1(s)$ of the depth loop and unity feedback depth loop controller $C_1(s)$ as

$$G_1(s)=-\frac{1}{s} \tag{54}$$

$$C_1(s)=-\frac{(\lambda s+1)(0.4s+1)[(3\bar{\lambda}+0.8)s+1]}{0.4\bar{\lambda}^3s^3+(1.2\bar{\lambda}^2+\bar{\lambda}^3)s^2+(2.4\bar{\lambda}+3\bar{\lambda}^2+0.32)s}. \tag{55}$$

The initial conditions of the vehicle are chosen as $z(0)=0m$ and $\theta(0)=0\text{deg}$. Applying the aforementioned setting, we measure the unit step input responses of the proposed control strategy. To demonstrate the output disturbances rejection capability of the designed control strategy, unit step output disturbances d and d_1 are added to the pitch and depth loops at $500s$ and $900s$, respectively.

Here, comparisons of control performances are made between the robust H_2 optimal control strategy proposed in this study and the controller proposed in Prestero (2001). The controller proposed in Prestero (2001) is consisted of an inner PD pitch loop and an outer proportional depth loop. We present simulation results for two cases. The first case is with the assumption that the vehicle dynamic model is accurate and it is equal to its nominal dynamic model. The second case is with the assumption that the vehicle dynamic model is uncertain and the uncertain vehicle dynamic model is created by introducing parametric uncertainties. We proceed as follows.

4.1. Simulations in the absence of the model uncertainties

In this case, it is assumed that there are no uncertainties in the vehicle dynamic model and thus the actual vehicle dynamic model is equal to its nominal dynamic model. The robust H_2 optimal pitch and depth loop controllers (53) and (55) proposed in this study and the pitch-and-depth loop PD depth controller presented in Prestero (2001) are simulated simultaneously to demonstrate the effectiveness of the proposed control strategy. For the robust H_2 optimal control strategy proposed in this study, the filter parameter values of λ and $\bar{\lambda}$ are founded as $\lambda=10.2$ and $\bar{\lambda}=15.8$. For the controller proposed in Prestero (2001), the proportional and derivative gains for the pitch loop PD controller are chosen as $K_p=0.21$ and $\tau_d=2$ and the proportional gain for the depth loop proportional controller is chosen as $\gamma=-1.3$. The above control gains are selected by trial and error. The obtained results are shown in Fig. 4.

Fig. 4 illustrates the step responses of the nominal vehicle dynamic system under the action of the robust H_2 optimal control strategy and

the controller proposed in Prestero (2001). Figs. 4 (a), (c), and (e) present the response results with the robust H_2 optimal control strategy. Figs. 4 (b), (d), and (f) present the response results with the controller proposed in Prestero (2001). From Figs. 4 (a)-(d), it can be seen that both control methods provide precise tracking for the nominal system before adding the output disturbances. But after adding the output disturbances at the instants $500s$ and $900s$, it is observed in Figs. 4 (a)-(d) that the robust H_2 optimal control strategy effectively rejects the output disturbances in both pitch and depth loops and still guarantees precise tracking, while the controller proposed in Prestero (2001) can not effectively reject the output disturbance in pitch loop, which leads to non-zero steady-state depth error (about $0.6m$). In addition, it is also seen in Figs. 4 (a)-(d) that although the settling time is shorter for the controller proposed in Prestero (2001) than for the robust H_2 optimal control strategy, there is serious oscillatory behaviour for the controller proposed in Prestero (2001) before system settling.

Figs. 4 (e) and (f) plot the fin angles of the vehicle with respect to the nominal vehicle dynamic system under the action of the robust H_2 optimal control strategy and the controller proposed in Prestero (2001). Fig. 4 (e) shows the response curve of the fin angle with the robust H_2 optimal control strategy. Fig. 4 (f) shows the response curve of the fin angle with the controller proposed in Prestero (2001). As observed in the two figures, too large fin angle is produced by the controller proposed in Prestero (2001) at the initial instant and the instants when the output disturbances are added (i.e., the instants $500s$ and $900s$) compared with the robust H_2 optimal control strategy. Such overlarge fin angle can not be achieved in practical applications due to the limit of the saturation.

4.2. Simulations in the presence of the model uncertainties

To reflect the robustness of the proposed control strategy against model uncertainties, an uncertain model of the depth-plane dynamics of the AUV is considered in this case. The uncertain vehicle dynamic model is created by introducing parametric uncertainties. Here as in Nag et al. (2013), it is assumed that the estimation uncertainty of the fin lift moment M_{δ_s} is 20% of its nominal value, the uncertainties in the values of added mass term $M_{\dot{q}}$ and hydrostatic moment M_{θ} are 25% of their respective nominal values. Meanwhile, the uncertainty in the value of velocity U is assumed to be 10% of its nominal value. The robust H_2 optimal pitch and depth loop controllers (53) and (55) generated based on the nominal dynamic model are utilized to deal with the uncertainties. The control gains for the robust H_2 optimal control strategy of this study and the controller of Prestero (2001) are taken the same values as in the first case. The obtained results are shown in Figs. 5 and 6.

Fig. 5 displays the step responses of the uncertain vehicle dynamic system under the action of the robust H_2 optimal control strategy and the controller proposed in Prestero (2001). The response results with the robust H_2 optimal control strategy are plotted in Figs. 5 (a), (c), and (e). The response results with the controller proposed in Prestero (2001) are plotted in Figs. 5 (b), (d), and (f). Comparing Fig. 5 with Fig. 4, it is clearly seen that the controller proposed in Prestero (2001) gives more oscillation and worse tracking accuracy under the model uncertainties, while the proposed robust H_2 optimal control strategy is rarely affected by the model uncertainties and thus shows better robustness than the controller proposed in Prestero (2001). Also as in the first case, it is observed in Figs. 5 (e) and (f) that the fin angle for the controller proposed in Prestero (2001) is too large at the initial instant and the instants $500s$ and $900s$, which is not suitable for practical engineering. The verification of the robust stability of pitch and depth loops with the robust H_2 optimal control strategy is shown in Fig. 6. It is clearly seen from Figs. 6 (a) and (b) that $T(s) < 1/\Delta_m(s)$ and $T_1(s) < 1/\Delta_{1m}(s)$. Thus, the pitch and depth closed-loop systems are robust stable.

5. Conclusions

For the depth-plane motion control problem of an AUV with output disturbances and time delay, a robust H_2 optimal control strategy is proposed in this paper. The kinematic and dynamic models of the AUV are firstly described using the inertial and body-fixed reference frames. For efficient controller design in practical applications, it is essential to consider a linear and reduced-order model. Thus, a linearized and reduced-order model of the AUV is then derived using the depth-plane dynamics of the AUV. Based on this linearized and reduced-order model, a robust H_2 optimal control method is developed. The developed control method can effectively deal with the time delay as well as the output disturbances and guarantees desired tracking. Considering that the uncertainties exist in the AUV dynamic model due to the changing operating conditions, the robust stability and robust performance of the proposed control method are discussed. Simulations are performed on the REMUS AUV. The results confirm the effectiveness of the proposed control approach on dealing with the output disturbances, time delay as well as model uncertainties, and verify the improved performances of the proposed control approach, namely higher tracking accuracy, better output disturbances rejection ability, stronger robustness against model uncertainties, and smaller fin angle input over the pitch-and-depth loop PD depth controller presented in Prestero (2001).

Acknowledgments

This work is partly supported by the National Natural Science Foundation of China (61473183, U1509211), National Postdoctoral Innovative Talent Program (BX201600103), China Postdoctoral Science Foundation (2016M601600), China Scholarship Council Foundation.

References

Campa, G., Wilkie, J., Innocenti, M., 1998. Robust control and analysis of a towed underwater vehicle. Int. J. Adapt. Contr. Signal Process. 12 (8), 689–716.
Cutipa-Luque, J.C., Donha, D.C., 2011. AUV identification and robust control. In: Proceedings of the 18th IFAC World Congress, Milano, Italy, vol. 18. pp. 14735–14741 PART 1.
Do, K.D., Pan, J., 2009. Control of Ships and Underwater Vehicles: Design for Underactuated and Nonlinear Marine Systems. Springer, Science & Business Media.
Feng, Z., Allen, R., 2004. Reduced order H_∞ control of an autonomous underwater vehicle. Contr. Eng. Pract. 12 (12 SPEC. ISS.), 1511–1520.
Fossen, T.I., 2011. Handbook of Marine Craft Hydrodynamics and Motion Control. Wiley, Chichester, West Sussex, UK.
Jalving, B., 1994. The NDRE-AUV flight control system. IEEE J. Ocean. Eng. 19 (4), 497–501.
Li, H., Yan, W., 2017. Model predictive stabilization of constrained underactuated autonomous underwater vehicles with guaranteed feasibility and stability. IEEE ASME Trans. Mechatron. 22 (3), 1185–1194.
Majohr, J., Buch, T., 2006. Modelling, simulation and control of an autonomous surface marine vehicle for surveying applications Measuring Dolphin MESSIN. In Advances in unmanned marine vehicles. IEE Control Series 329–352.
Milliken, L.G., 1984. Multivariable Control of an Underwater Vehicle. Master's Thesis. Massachusetts Institute of Technology.
Morari, M., Zafiriou, E., 1989. Robust Process Control. Prentice Hall International.
Moreira, L., Soares, C.G., 2008. H_2 and H_∞ designs for diving and course control of an autonomous underwater vehicle in presence of waves. IEEE J. Ocean. Eng. 33 (2), 69–88.
Nag, A., Patel, S.S., Kishore, K., Akbar, S.A., 2013. A robust H-infinity based depth control of an autonomous underwater vehicle. In: Proceedings of the 2013 International Conference on Advanced Electronic Systems, Pilani, India, pp. 68–73.
Petersen, I.R., Ugrinovskii, V.A., Savkin, A.V., 2000. Robust Control Design Using H_∞ Methods. Springer Verlag.
Prestero, T., 2001. Verification of a Six-degree of Freedom Simulation Model for the REMUS Autonomous Underwater Vehicle. Ph.D. Thesis. Massachusetts Institute of Technology.
Qiao, L., Zhang, W., 2017. Adaptive non-singular integral terminal sliding mode tracking control for autonomous underwater vehicles. IET Control Theory & Appl. 11 (8), 1293–1306.
Qiao, L., Yi, B., Wu, D., Zhang, W., 2017. Design of three exponentially convergent robust controllers for the trajectory tracking of autonomous underwater vehicles. Ocean Eng. 134, 157–172.
Qiao, L., Zhang, W., 2018a. Double-loop integral terminal sliding mode tracking control for UUVs with adaptive dynamic compensation of uncertainties and disturbances. IEEE J. Ocean. Eng. https://doi.org/10.1109/JOE.2017.2777638. online.

Qiao, L., Zhang, W., 2018b. Adaptive second-order fast nonsingular terminal sliding mode tracking control for fully actuated autonomous underwater vehicles. IEEE J. Ocean. Eng. https://doi.org/10.1109/JOE.2017.2777638. online.
Santhakumar, M., Asokan, T., 2013. Power efficient dynamic station keeping control of a flat-fish type autonomous underwater vehicle through design modifications of thruster configuration. Ocean Eng. 58, 11–21.
Shen, C., Buckham, B., Shi, Y., 2017. Modified C/GMRES algorithm for fast nonlinear model predictive tracking control of AUVs. IEEE Trans. Contr. Syst. Technol. 25 (5), 1896–1904.
Shojaei, K., Arefi, M.M., 2015. On the neuro-adaptive feedback linearising control of underactuated autonomous underwater vehicles in three-dimensional space. IET Control Theory & Appl. 9 (8), 246–258.
Silvestre, C., Pascoal, A., 2007. Depth control of the INFANTE AUV using gain-scheduled reduced order output feedback. Contr. Eng. Pract. 15 (7), 883–895.
SNAME, 1950. Nomenclature for Treating the Motion of a Submerged Body through a Fluid. Technical Report Bulletin 1–5. Society of Naval Architects and Marine Engineers, NY, USA.
von Alt, C., Grassle, J.F., 1992. LEO-15: an unmanned long term environmental observatory. In: Proceedings of MTS/IEEE Oceans Conference, Newport, RI, vol. 2. pp. 849–854.
von Alt, C., Allen, B., Austin, T., Stokey, R., 1994. Remote environmental monitoring units. In: Proceedings of MTS/IEEE Oceans Conference, Cambridge, MA.
Wadoo, S.A., Sapkota, S., Chagachagere, K., 2012. Optimal control of an autonomous underwater vehicle. In: Proceedings of 2012 IEEE Long Island Systems, Applications and Technology Conference, Farrmingdale, NY, United States, pp. 1–6.
Wang, Y., Bai, L., Liu, S., 2014. Robust H2/H∞ control of nonlinear system with differential uncertainty. In: Proceedings of 2014 IEEE Conference and Expo Transportation Electrification Asia-Pacific (ITEC Asia-Pacific), Beijing, China, pp. 1–6.
Wang, Y., Gu, L., Gao, M., Zhu, K., 2016. Multivariable output feedback adaptive terminal sliding mode control for underwater vehicles. Asian J. Contr. 18 (1), 247–265.
Xiang, X., Lapierre, L., Jouvencel, B., 2015. Smooth transition of AUV motion control: from fully-actuated to under actuated configuration. Rob. Autom. Syst 67, 14–22.
Yan, Z., Yu, H., Zhang, W., Li, B., Zhou, J., 2015. Globally finite-time stable tracking control of underactuated UUVs. Ocean Eng. 107, 132–146.
Zhang, F., Marani, G., Smith, R.N., Choi, H.T., 2015. Future trends in marine robotics. IEEE Robot. Autom. Mag. 22 (1), 14–21 122.
Zhang, W., Ou, L., Gu, D., 2006. Algebraic solution to H_2 control problems. I. The scalar case. Ind. Eng. Chem. Res. 45 (21), 7151–7162.
Zhang, W., 2011. Quantitative Process Control Theory. CRC Press.
Zhang, X., Han, Y., Bai, T., Wei, Y., Ma, K., 2016. H_∞ controller design using LMIs for high-speed underwater vehicles in presence of uncertainties and disturbances. Ocean Eng. 104, 359–369.
Zhang, X., Ma, K., Wei, Y., Han, Y., 2017. Finite-time robust H_∞ control for high-speed underwater vehicles subject to parametric uncertainties and disturbances. J. Mar. Sci. Technol. 22 (2), 201–218.
Zhou, J., Bian, X., Zhang, W., Tang, Z., 2011. Current profile data aided positioning for autonomous underwater vehicles. In: Proceedings of MTS/IEEE Oceans Conference, pp. 1–5 Kona, HI.
Zhou, K.M., 1998. Essentials of Robust Control. Prentice Hall, Upper Saddle River, NJ.